Analytica Chimica Acta 1143 (2021) 37–44

Contents lists available at ScienceDirect

Analytica Chimica Acta

journal homepage: www.elsevier.com/locate/aca

Detection of phospholipase A_2 in serum based on LRET mechanism between upconversion nanoparticles and SYBR green I

Dengwang Luo [a, 1], Chaoyu Zhang [b, 1], Yao Fang [a], Yiping Shen [a], Yuan Liang [a], Yaokun Xia [a], Fang Wu [a], Xiaosong Chen [b], Jingrong Liu [c], Jinghua Chen [a, d, **], Chunyan Li [a, d, ***], Jianming Lan [a, d, *]

[a] The School of Pharmacy, Fujian Medical University, Fuzhou, Fujian, 350108, PR China
[b] Department of Plastic Surgery, The Union Hospital of Fujian Medical University, Fuzhou, Fujian, 350001, PR China
[c] Affiliated Fuzhou First Hospital of Fujian Medical University, Fuzhou, Fujian, 350009, PR China
[d] Key Laboratory of Drug Target Discovery and Structural and Functional Research, Fuzhou, Fujian, 350108, PR China

HIGHLIGHTS

- A detection technology based on LRET from UCNPs to SG was designed.
- UCNPs acted as the LRET donor can effectively eliminate the background interference from biological samples.
- The biosensor effectively utilizes the recognition function of SG for dsDNA.
- The ratio fluorescent approach for testing PLA_2 has high sensitivity and wide linearity range.

GRAPHICAL ABSTRACT

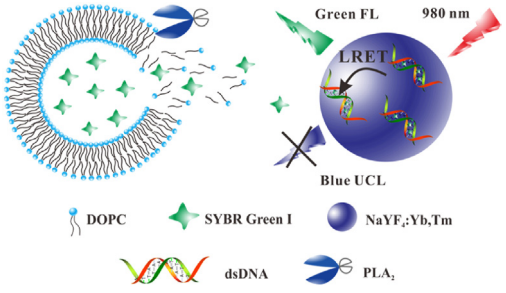

ARTICLE INFO

Article history:
Received 5 August 2020
Received in revised form
18 November 2020
Accepted 20 November 2020
Available online 24 November 2020

Keywords:
Phospholipase A_2
Luminescence resonance energy transfer
Upconversion nanoparticle
SYBR Green I
Double-stranded DNA
Liposome

ABSTRACT

Phospholipase A_2 (PLA_2) may be a vital biomarker for the prediction and diagnosis of some diseases. Consequently, it is of great significance to quantitatively detect PLA_2 in biologic samples. Herein, on the basis of the principle of luminescence resonance energy transfer (LRET) between upconversion nanoparticles (UCNPs) and SYBR Green I (SG), we proposed a technology for the highly sensitive detection of PLA_2 amount. Therein, as an energy receptor, SG will be quantitatively loaded into liposomes firstly. Then, due to the hydrolysis of liposomes under the catalysis of PLA_2, SG will be released and inserted into the double-stranded DNA (dsDNA) on the surface of UCNPs, which triggers the LRET because of the shortening of effective spatial distance between UCNPs and SG. Under exciting of NIR light, UCNPs emit luminescence at 476 nm, which makes SG emit fluorescence at 522 nm through LRET. Under optimal conditions, the emission intensity ratio ($I_{522\ nm}/I_{476\ nm}$) increased linearly with the PLA_2 amount in the range of 20 U/L to 400 U/L, and the limit of detection (LOD) reached 15 U/L. Here, after comparing with the clinical standard method, it is found that the biosensor is expected to provide a convenient and sensitive assay for the detection of PLA_2 in actual serum samples. Furthermore, such biosensor can also be used to test the inhibitor of PLA_2.

* Corresponding author. The School of Pharmacy, Fujian Medical University, Fuzhou, Fujian, 350108, PR China.
** Corresponding author. The School of Pharmacy, Fujian Medical University, Fuzhou, Fujian, 350108, PR China.
*** Corresponding author. The School of Pharmacy, Fujian Medical University, Fuzhou, Fujian, 350108, PR China.
E-mail addresses: cjh_huaxue@126.com (J. Chen), cyli65@126.com (C. Li), jianminglan@fjmu.edu.cn (J. Lan).
[1] Dengwang Luo and Chaoyu Zhang make equal contribution to this paper.

https://doi.org/10.1016/j.aca.2020.11.025
0003-2670/

1. Introduction

Phospholipase A_2 (PLA_2) is a kind of hydrolase which can catalyze acyl group in the sn-2 position of glycerol phospholipid [1], which widely distributes in animal and plant tissues, bacteria and cell nuclear secretions, involving in physiological processes such as inflammation, membrane remodeling, intercellular signal transduction, lipid peroxidation repair and host response, etc. PLA_2 plays a crucial role in regulating the balance of phospholipid in vivo, controlling the metabolism and growth of the body, and participating in the pathological process of diseases. Recent studies have shown that PLA_2 may act as a latent biomarker for disease diagnosis. The increasing of PLA_2 activity is closely related to atherosclerosis [2,3], rheumatoid arthritis [4], acute sepsis [5] and cancer [6,7]. Therefore, it is very significant to analyze and detect PLA_2 activity for the early diagnosis and prognosis analysis of related diseases.

Recently, many efforts have been made to determine the activity of PLA_2, including colorimetric assay [8,9], magnetic relaxation assay [10,11], electrochemical sensor [12], radiometric-based assay [13,14], enzyme-linked immunoassay [15], surface plasmon resonance [16], etc. However, these assays often suffer from limitations such as low sensitivity, complex sample processing, poor stability and high cost. Fluorescence assay is widely used in PLA_2 detection because of its high sensitivity, good stability, simple operation and rapid detection. To date, many researchers have employed fluorescent probes to monitor enzyme activity in real time. Fluorescence resonance energy transfer (FRET) is one of the most popular fluorescence analysis methods for detecting PLA_2 activity. FRET is the process of transferring the energy generated by the fluorophore donor to the fluorophore acceptor in a non-radiative manner, which results in the fluorescence quenching of the fluorophore donor [17].

According to the structural features, PLA_2 can catalyze the hydrolysis of phospholipids at lipid interface, including micelle, monolayer and bilayer phospholipid aggregates [18]. Researchers have constructed a number of FRET-based fluorescence sensing assays for the detection of PLA_2 activity. For instance, Wichmann et al. designed a kind of small-molecule FRET probe based on 7-nitrobenzo-2-oxa-1,3-diazole amine (NBD) and Nile red as energy donor and acceptor, respectively, for real-time testing of PLA_2 activity in cells and organisms [19]. Li et al. also exploited a fluorescent probe based on the Quantum dot cluster (QDC) encapsulated in phospholipid micelle for the PLA_2 activity assay [20]. However, the above methods usually need to couple fluorophores with phospholipids to obtain functionalized fluorescence probes, which increases the detection steps and cost. Therefore, the design of a label-free fluorescence assay based on liposomal nanoprobes for the detection of PLA_2 activity will effectively simplify the experimental procedure and reduce cost.

The hydrophilic inner cavity of liposomes can be virtually applied to capture nearly all of the water-soluble signal molecules, such as fluorophores [21], enzymes [22] and electroactive molecules [23]. Using liposome as a carrier, it can enrich signal molecules to amplify signal and enhance sensitivity to the target. SG, an excellent fluorescent dye embedded in DNA strands, exhibits higher binding affinity and more strong fluorescence toward dsDNA than that in single-stranded (ssDNA) [24,25]. Compared with acridine dyes such as ethidium bromide (EB), SG has higher sensitivity and lower toxicity. In addition, compared with asymmetric cyanine dyes such as TOTO (thiazole orange isomeric dimer) and YOYO (oxazole yellow isomeric dimer), SG overcomes the problems of expensive price, poor solubility and photobleach [26,27]. These properties make SG feasible in label-free biosensors. Based on the above advantages, SG can be loaded into liposomes as a label-free fluorescence probe, combining suitable energy donor to establish the FRET system, which is expected to be promising for the detection of PLA_2 activity. Rare-earth doped UCNPs have a broad prospect in biomedical field owing to their unparalleled performance, including NIR light excitation, large anti-Stokes shifts, good chemical and optical stability, low background fluorescence and large optical penetration depth [28–30]. Especially, as energy donors of luminescence resonance energy transfer (LRET), UCNPs can also protect energy receptors from being directly excited, so as to effectively eliminate the background disturbance from complicated biological samples, and thus realize the sensitive detection of high signal-to-noise ratio. So far, researchers have developed a variety of upconversion luminescence (UCL) biosensors by using UCNPs as energy donors to detect metal ions [31], small biological molecules [32], RNA [33], toxins [34], etc., with satisfactory results.

Inspired by the above researches, we put forward a LRET strategy based on DNA-coated UCNPs and liposomes-loaded SG for the detection of PLA_2 amount. This assay is promising to be a convenient and sensitive biosensor for monitoring PLA_2 and testing enzyme inhibitor.

2. Experimental

2.1. Materials and reagents

Rare-earth oxides, used for the synthesis of stearate precursors, including yttrium oxide (Y_2O_3, 99.999%), thulium oxide (Tm_2O_3, 99.999%), and ytterbium oxide (Yb_2O_3, 99.999%), oleic acid (OA, 85%), 1-Octadecene (ODE, 90%), 1, 2-dioleoyl-sn-glycero-3-phosphocholine (DOPC, 99%) and N,N-Dimethylformamide (DMF) were purchased from Aladdin (Shanghai, China). SYBR Green I (SG), sodium fluoride (NaF), octadecanoic acid ($C_{17}H_{35}COOH$), Tris(hydroxymethyl)methyl aminomethane (Tris), calcium chloride ($CaCl_2$) and ethylenediaminetetraacetic acid (EDTA) were purchased from Sinopharm (Beijing, China). Sephadex G-50 (medium) was purchased from Solarbio (Beijing, China). Nitrosonium tetrafluoroborate ($NOBF_4$) was purchased from InnoChem (Beijing, China). Phospholipase A_2 (PLA_2), phospholipase C (PLC), phospholipase D (PLD), alkaline phosphatase (ALP), α-glucosidase, proteinase K, lysozyme, catalase, urease and acetyl cholinesterase (AchE) were purchased from Sigma-Aldrich (Australia). All DNA sequences (ESI 1) were obtained from Sangon (Shanghai, China). The rest of the reagents are analytical reagent grade, not further purified. Ultrapure water with 18.2 MΩ•cm was used in all aqueous solution.

2.2. Apparatus and characterization

The morphology of UCNPs and liposomes was characterized by the JEM-2100F transmission electron microscope (JEOL, Japan). The crystalline phase of UCNPs was determined by the MiniFlex600 X-ray powder diffractometer (Riguka, Japan). The luminescence decay curve of UCNPs was measured by the FLS980 Series of Fluorescence Spectrometers (PL, UK). The functional groups on the surface of UCNPs were confirmed by the Perkin2 Elmer Spectrum 2000 infrared spectroscopy (PE, USA). The luminescence spectra of UCNPs were recorded by the Cary Eclipse fluorescence spectrophotometer (Agilent Technologies, USA) equipped with an external 980 nm laser. The ultraviolet–visible (UV–Vis) absorption spectra of UCNPs were recorded by the Cary-60 spectrophotometer (Agilent Technologies, USA). The dynamic light scattering (DLS) analyses and Zeta potentials of liposomes and UCNPs were collected by the Litesizer™ 500 nanoparticle size and Zeta potential analyzer (Anton Paar, Austria). Lipoprotein-associated phospholipase A_2 kit (Lp-PLA_2 kit) was tested by Beckman AU5800 automatic biochemical analyzer (Meikang Biotechnology Co., Ltd, China).

2.3. Preparation of oleic acid-coated β-$NaYF_4$:Yb,Tm UCNPs

Oleic acid-coated β-$NaYF_4$:Yb,Tm UCNPs (OA-UCNPs) were synthesized by a improved thermal decomposition method [35]. In brief, 0.8 mmol $Ln(C_{17}H_{35}COO)_3$ (Y: Yb: Tm = 76.5%, 23%, 0.5%), 28 mmol NaF, 12 mL ODE and 8 mL OA were added to a suitable three-necked flask. Under argon flow, the mixture was heated to 140 °C to expel water, with strong stirring for 40 min. Subsequently, the mixture was rapidly heated to 315 °C under argon flow with steadily stirring for 40 min. Next, the resulting product was naturally cooled to ambient temperature. The synthesized product was precipitated by anhydrous ethanol and the supernatant was discarded after centrifugation. Then, the resulting UCNPs were washed repeatedly with cyclohexane/anhydrous ethanol (volume ratio, 3:1) to remove excess OA, and washed with ultrapure water to remove excess NaF for several times. Finally, the UCNPs were dried in vacuum for subsequent study.

2.4. Preparation of dsDNA-modified UCNPs

To prepare dsDNA-modified UCNPs (dsDNA-UCNPs), a two-step ligand exchange reaction on the surface of UCNPs was processed on the basis of a reported method [36]. In the first step, 5 mL of OA-UCNPs hexane-dispersion (10 mg/mL) was mixed with 5 mL of $NOBF_4$ DMF-solution (0.01 M). The mixture was treated by sonication for 30 min, causing the transfer of UCNPs from the upper hexane layer into the lower DMF layer. The dispersed UCNPs in DMF were flocculated by adding toluene/hexane (volume ratio, 1:1). After centrifugation, the precipitated BF_4^--UCNPs were collected and dried in vacuum at 60 °C. Then, BF_4^--UCNPs were dispersed in Tris-HCl buffer I (10 mM, pH 8.0, 15 mM $CaCl_2$, 150 mM NaCl), with formulated concentration of 1 mg/mL. In the second step, 5 nmol of 30A and 30T were added into 5 mL BF_4^--UCNPs dispersion, respectively. The dispersion was stirred slowly overnight at 4 °C. The dsDNA-UCNPs were gathered by ultrafiltration centrifugation, washed repeatedly with ultrapure water, and dispersed again in 5 mL Tris-HCl buffer I at 4 °C for next experiment.

2.5. Preparation of SG-loaded liposomes

SG-loaded liposomes were synthesized by utilizing the film hydration/extrusion process as previously described [37]. The process of experimental operation was shown in ESI 2. In brief, DOPC (0.025 mmol) was dissolved in 5 mL mixture of chloroform/methanol (v/v = 4/1). Subsequently, the above mixture was transfer into a round-bottomed flask and dried in a rotary evaporator for 30 min at 40 °C, forming a uniform lipid membrane on the inner surface of flask. The residual organic solvents were removed under argon flow and the lipid membrance was dried in vacuum overnight. Then, this lipid membrance was hydrated with 2.5 mL of Tris-HCl buffer II (10 mM, pH 8.0, 2 mM EDTA) solution containing 50 μM SG in a water bath (50 °C) for 30 min, the SG-loaded liposomes were obtained through vortex and sonication for 20 min. In order to improve the encapsulation efficiency, the liposome suspension was squeezed out for 9 times through the 100 nm model polycarbonate membrane by using a stainless-steel extruder (Avanti polar lipids). Unencapsulated SG was removed by size exclusion chromatography (Sephadex G-50 column) using Tris-HCl buffer II solution as eluent. The obtained SG-loaded liposomes were stored at 4 °C.

2.6. Determination of PLA_2 amount based on LRET

100 μL of 2.6 μM SG-loaded liposomes (the determination of SG concentration in liposomes was shown in ESI 3) was mingled by 100 μL dsDNA-UCNPs (1 mg/mL). Then, 2 μL PLA_2 solutions (final concentrations from 0 to 2000 U/L) were prepared by different amounts of Tris-HCl buffer III (10 mM, pH 7.7, 2 mM EDTA, 150 mM NaCl), respectively. After that, each mixture was incubated for 80 min at 37 °C. Finally, the UCL of the resulting mixtures were tested under the excitation of 980 nm NIR light, and the excitation power density is 1.47 W/cm^2 (ESI 4). To test the selectivity of the nanoprobe for PLA_2, UCL was further tested under the same conditions after replacing PLA_2 with other biomolecules.

2.7. Testing of PLA_2 inhibitor

For the inhibitor assay, various concentrations of LY311727 (0–100 μM) and PLA_2 (500 U/L) were pre-incubated in 10 μL of Tris-HCl buffer II for 20 min at 37 °C, and then the same procedures of UCL detection were carried out.

2.8. Testing of PLA_2 amount in human serum samples

The human plasma samples (From healthy persons and patients with coronary heart disease, pneumonia, and cholelithiasis) were provided by the Union Hospital of Fujian Medical University. To eliminate the interfering proteins, the human plasma samples had been centrifuged before testing. Firstly, the healthy human serums were centrifuged at 5729 g for 10 min. Then according to section 2.6, the standard addition method of the proposed biosensor was used to verify the feasibility of PLA_2 detection in healthy human serum. Secondly, the all serums were centrifuged at 890 g for 5 min, and we used standard Lp-PLA_2 kit and our proposed biosensor to detect the amount of PLA_2 in the serums of healthy persons and different patients, respectively, and then compared the results.

3. Results and discussion

3.1. Test mechanism of PLA_2 amount

Based on the LRET between dsDNA-UCNPs and liposomes-loaded SG, a label-free UCL biosensor was constructed to detect PLA_2 amount. The detection principle of PLA_2 amount was shown in Fig. 1. In the detection system, SG was encapsulated in a closed cavity of the liposome, and the surface of UCNPs was modified with dsDNA. In the absence of PLA_2, UCNPs emitted intense blue UCL under excitation by 980 nm NIR light. Next, under the catalysis of PLA_2, the encapsulated SG would be released from liposomes due to enzymatic cleavage of glycerol phospholipid sn-2 ester bond. The released SG was subsequently inserted into the small grooves of dsDNA on the surface of UCNPs. Thus, the acceptors (SG) and donors (UCNPs) would get close, making the quenching of blue UCL (476 nm) from UCNPs and the emission of green fluorescence (522 nm) from SG due to their highly overlapped spectrum. As a result, quantitative detection of PLA_2 amount was achieved by the change of the $I_{522\ nm}/I_{476\ nm}$ ratio, according to the effect of PLA_2 concentration on LRET.

3.2. Synthesis and characterization of dsDNA-UCNPs

TEM image of OA-UCNPs (Fig. 2A) shows that UCNPs are evenly dispersed, with an average size of about 25 nm. UCNPs are of fine single crystalline morphology (Fig. 2A, inset). The lattice fringe belonging to the (100) lattice plane can be apparently identified through HRTEM image, which is about 0.517 nm. Spotty polycrystalline diffraction rings corresponding with the hexagonal phase (β) $NaYF_4$ lattice are showed in the selected area electron diffraction (SAED) pattern (Fig. 2B). Besides, the XRD pattern of UCNPs (Fig. 2C) is consistent with the standard pattern of β-$NaYF_4$

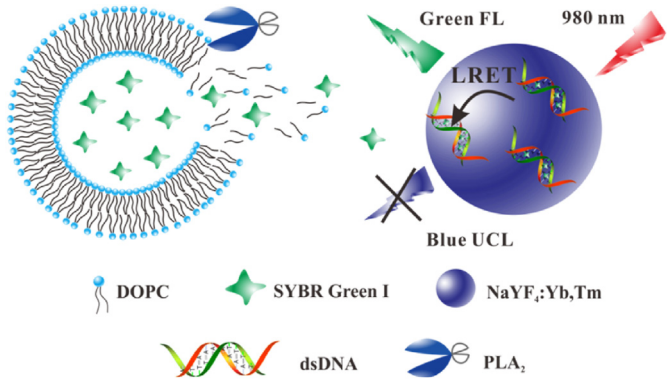

Fig. 1. The mechanism of PLA_2 detection based on the LRET between UCNPs and SG.

(JCPDS: 28–1192), indicating that the synthesized UCNPs belong to the hexagonal nanocrystals.

In order to obtain positively charged UCNPs for direct dsDNA attaching, the oleate ligands attaching to the surface of UCNPs were removed by $NOBF_4$ treatment. To be specific, NO^+ could easily react with solvated water molecules to create a fairly acidic environment, which facilitated protonation to remove the surface ligands [36], thus contributing to the coordination between the positively charged Ln^{3+} ions and BF_4^- anions. As shown in FT-IR spectra (Fig. 2D), after the replacement of inorganic BF_4^- anions, the intensity of the representative C–H stretching vibration ascribed to OA molecules at 2800-3000 cm^{-1} was noticeably reduced, a new peak ascribed to BF_4^- anions at 1082 cm^{-1} was observed. Obviously, the remaining peaks at 1655 and 1384 cm^{-1} belonged to C=O stretching vibration and characteristic peak of methyl group ($-CH_3$) of DMF molecules, respectively. The typical DNA absorption band appeared at 260 nm in UV–Vis absorption spectrum (Fig. 2E) indicated that dsDNA successfully adhered to the surface of UCNPs. Fig. 2F showed that the Zeta potentials of UCNPs changed from −15.56 mV to +32.65 mV because of the exposing of positively charged Ln^{3+} ions, and then reduced to −18.50 mV on account of the coordination between Ln^{3+} ions on the surface of UCNPs and the negatively charged phosphate skeletons of DNA [38].

Finally, through quantitative analysis, the result indicates that the ratio between UCNPs and dsDNA is approximately 1:13, suggesting the concentration of acceptor is much higher than donor (ESI 5). Furthermore, it is verified by the UCL analysis that the SG dye has LRET effect only when it is intercalated on the small grooves of dsDNA on the surface of UCNPs (ESI 6).

3.3. Preparation and characterization of SG-loaded liposomes

SG dyes were encapsulated into liposomes through the film hydration/extrusion process. To reduce background signal, unencapsulated SG should be removed as much as possible.

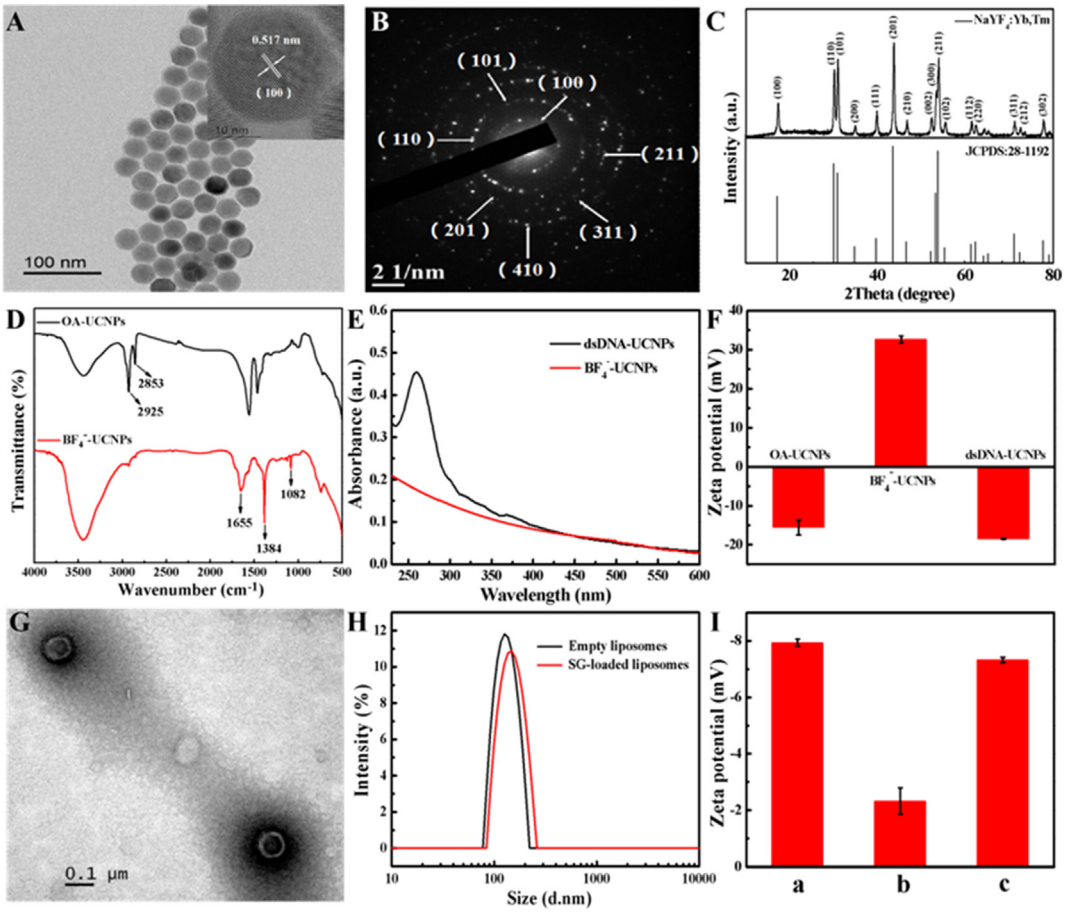

Fig. 2. (A) TEM image of UCNPs (Inset: HRTEM image of UCNPs). (B) SAED pattern of UCNPs. (C) XRD pattern of UCNPs. (D) FT-IR spectra of OA-UCNPs and BF_4^--UCNPs. (E) UV–Vis absorption spectra of BF_4^--UCNPs and dsDNA-UCNPs. (F) Zeta potentials of OA-UCNPs, BF_4^--UCNPs and dsDNA-UCNPs. (G) TEM image of SG-loaded liposomes. (H) Dynamic light scattering of empty liposomes and SG-loaded liposomes. (I) Zeta potentials of empty liposomes (a), SG-loaded liposomes without purifying (b) and SG-loaded liposomes with purifying (c).

Consequently, we explored the optimal separation method between liposomes and unencapsulated SG. The results indicated the column chromatography could ensure the integrity and homogeneity of liposomes to the utmost extent, which was most suitable for this experiment comparing with other separation methods (ESI 7). To enrich more SG-loaded liposomes, we selected Sephadex G-50 column with a length of 4 cm for subsequent experiments (ESI 8). To determine the accurate concentration of SG in liposomes, we employed 1% Triton X-100 as the optimal demulsifier that could demulsify the liposomes completely (ESI 9). To improve the encapsulation efficiency of SG, extrusion times were optimized, and various parameters were characterized (ESI 9). The results indicated the optimal number of extrusion was 9 times (ESI 10).

After purification, the morphology, granularity and electronegativity of SG-loaded liposomes were analyzed by TEM, DLS and Zeta potential, respectively. The TEM image (Fig. 2G) indicated that the resulting liposomes had distinct vesicle structures and uniform particle size. The DLS analyses of empty liposomes and SG-loaded liposomes (Fig. 2H) showed that the size of the liposomes ranged from 140 to 150 nm, demonstrating the uniform size distribution for liposomes before and after encapsulating SG. In addition, the Zeta potentials of empty liposomes and SG-loaded liposomes without purifying were −7.93 mV and −2.32 mV, respectively. That is because the external electric field generated by the membrane dipole potential causes the liposome consisting of zwitterionic DOPC to exhibit a negative surface potential [39]. When SG with positive potential adsorbed on the surface of liposomes, the charge was neutralized. After purification, the Zeta potential of SG-loaded liposomes became −7.32 mV (Fig. 2I). Obviously, the result indicated that unencapsulated SG had been almost removed from the surface of liposomes, which was beneficial to reduce background signal and avoid false positive result.

Furthermore, we had verified that there was no reabsorption of the blue light by the dye encapsulated into the liposome, and the light scattering from liposome had no effect on the light signal in liposome-UCNPs system (ESI 11). These showed that nanoprobes composed of such system were feasible.

3.4. Construction of the LRET-based nanoprobes

In the LRET system, UCNPs were used as the energy donors due to their unique optical performances. Excited by 980 nm NIR light, strong emissions of UCNPs appeared around 450 and 476 nm, which generated from $^1D_2$-$^3F_4$ and $^1G_4$-$^3H_6$ of Tm^{3+}, respectively. Chief of all, the 476 nm emission matched well with the absorption of SG dyes (Fig. 3A) that were used as the energy acceptors.

When SG-loaded liposomes were mixed in the solution containing dsDNA-UCNPs, in the absence of PLA_2, SG would not be released from liposomes. Therefore, UCNPs emitted blue UCL at 476 nm under excitating by 980 nm NIR light. Nevertheless, under the influence of PLA_2, the released SG would be close to UCNPs through inserting into the dsDNA. The blue UCL of UCNPs could be partly transferred to the nearby SG under excitating by 980 nm NIR light, leading to the fluorescence emission of SG at 522 nm (Fig. 3B). Thus, the PLA_2 activity could be quantified by the fluorescence intensity ratio ($I_{522\ nm}/I_{476\ nm}$). To achieve the optimum conditions for LRET between UCNPs and SG, the length and concentration of dsDNA sequences were optimized. As discussed in ESI 12, when the selected DNA sequence was 30AT with the concentration of 0.5 μM, the LRET achieved optimum efficiency.

In order to illuminate the LRET process, the luminescence decay curves and lifetimes of UCNPs linking with and without acceptor (SG) were tested. As shown in Fig. 3C, the luminescence lifetimes of UCNPs linking with and without SG were measured to be 520 μs and 443 μs, respectively. The LRET efficiency (E) related to the luminescence lifetimes of the donors (UCNPs) was shown as the following equation [40]:

$$E = 1 - \frac{\tau_{DA}}{\tau_D}$$

where τ_D and τ_{DA} were the luminescence lifetimes of donor in the absence and presence of the acceptor, respectively. In accordance with the above equation, the LRET efficiency was calculated to be 14.8%. The results of luminescence spectra and luminescence lifetimes showed that a biosensor based on UCNPs-SG for PLA_2 detection could be successfully constructed.

3.5. Detection of PLA_2 amount

We firstly tested the sensitivity of SG-loaded liposomal nanoprobes without UCNPs as the energy donors for the detection of PLA_2. The released SG could be inserted into the small grooves of dsDNA, which caused the fluorescence of SG to enhance significantly. Obviously, there was a fairly high fluorescent background in the SG-loaded liposomal nanoprobes for the assay of PLA_2 (Fig. 4A). As shown in Fig. 4B, a linear correlation was observed between the value of $(F-F_0)/F_0$ of SG-loaded liposomal nanoprobes and PLA_2 amount over the range of 50–250 U/L. The limit of detection for PLA_2 was 32 U/L (computed as 3 δ/S, where δ is the standard deviation of the control group and S is the slope of the linearity).

In addition, the LRET-based UCNPs-SG nanoprobes were explored for the detection of PLA_2 amount. The ratiometric fluorescence curves were tested for monitoring the hydrolysis reaction catalyzed by different concentrations of PLA_2 in real time (Fig. 5A). As the reaction time continued, the degree of hydrolysis gradually increased until reaching 80 min, which was selected as the optimal reaction time. Furthermore, in consideration of the vital function of Ca^{2+} ions in the hydrolysis reaction, the concentration of Ca^{2+} ions was further optimized. The result showed that PLA_2 had the highest amount with 7.5 mM Ca^{2+} ions in hydrolyzing SG-loaded liposomes (ESI 13).

Finally, the ability of the UCNPs-SG nanoprobes to quantify PLA_2 amount was studied. Fig. 5B showed UCL emission spectra of the UCNPs-SG nanoprobes after incubation with various concentrations of PLA_2. The result indicated that the fluorescence ratio almost reached maximum after adding 1000 U/L PLA_2 (Fig. 5C). Fig. 5D presented the linear relationship between the $I_{522\ nm}/I_{476\ nm}$ ratio and the concentration of PLA_2 in the range 20–400 U/L. The LOD of the biosensor for PLA_2 was as low as 15 U/L. Obviously, in the UCNPs-SG nanoprobes, $NaYF_4$:Yb,Tm UCNPs served as the energy donors, will effectively avoid autofluorescence and background fluorescence. Furthermore, the UCNPs-SG nanoprobes will provide a relatively lower LOD and a wide dynamic range.

ESI 14 shows the comparison of linear range and LOD of diverse analysis methods for PLA_2. Our method exhibits better analytical performance than most methods due to low background interference and stability. Notably, electrochemical analysis shows lower LOD than our method. Nevertheless, electrochemical analysis usually suffers from some inevitable defects, such as complex sample interference and poor reproducibility. According to the above analysis, the proposed method has the potential for quantification of PLA_2 amount in actual samples.

3.6. Selectivity of PLA_2 assay

For evaluating the selectivity of PLA_2 testing, some interfering substances such as urease, catalase, α-glucosidase, alkaline phosphatase, lysozyme, protease K, phospholipase C, phospholipase D, etc. were incubated with the mixture of UCNPs-SG nanoprobes

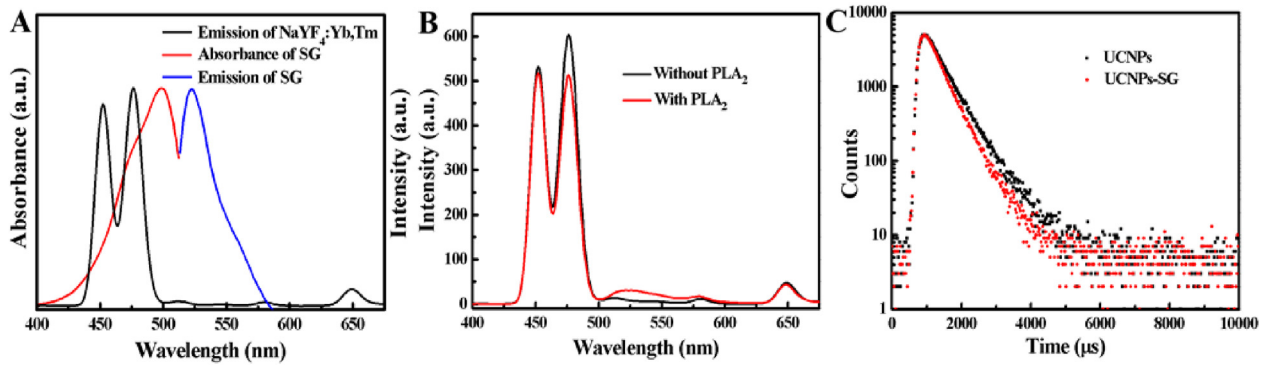

Fig. 3. (A) UV–Vis absorption spectrum (red line) and fluorescence emission spectrum (blue line) of SG, and UCL spectrum (black line) of UCNPs. (B) UCL spectra of UCNPs-SG nanoprobes before (black line) and after (red line) incubation with 500 U/L PLA_2. (C) UCL decay curves of UCNPs (black line) and UCNPs-SG (red line) at 476 nm upon excitation by 980 nm NIR light. (For interpretation of the references to color in this figure legend, the reader is referred to the Web version of this article.)

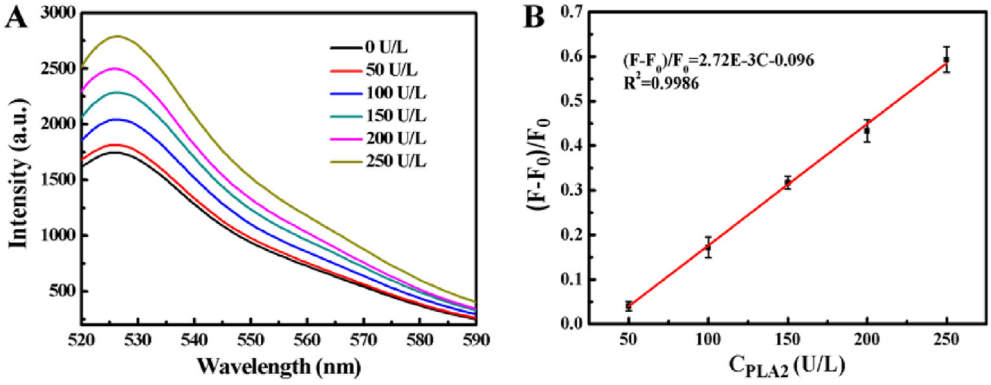

Fig. 4. (A) Fluorescence spectra of SG-loaded liposomal nanoprobes after incubation with different concentrations of PLA_2 (0, 50, 100, 150, 200, 250 U/L). (B) Linear range of the plot of $(F-F_0)/F_0$ at 522 nm against PLA_2 amount (50–250 U/L). F_0 and F are the fluorescence intensities of the SG-loaded liposomal nanoprobes in the absence and presence of PLA_2, respectively. Error bars represent the standard deviations from three replicated experiments.

under the optimum condition. In the test, the concentrations of PLA_2 and other interfering substances were 500 U/L and 1000 U/L, respectively. Fig. 6A shows that the above interfering enzymes do not affect the determination of PLA_2 in the system, indicating that the assay has a good specific response to PLA_2.

3.7. Inhibitory test of PLA_2

The function of the biosensor in the determination of enzyme inhibitor was further studied. LY311727, an inhibitor of phosphatidylcholine-specific PLA_2, was used for testing the inhibition level of PLA2 amount. As shown in Fig. 6B, the $I_{522\ nm}/I_{476\ nm}$ ratio decreased with the increasing of LY311727 concentration, manifesting that LY311727 could effectively inhibit PLA_2 amount. According to this research, the IC_{50} value was calculated to be 8.37 μM when the nanoprobes were incubated with 500 U/L PLA_2. Consequently, these results suggested that the proposed method had good potential for testing inhibitor of PLA_2.

3.8. Detection of PLA_2 amount in human serum samples

In order to evaluate whether the biosensor has potential application value in clinical analysis, PLA_2 amount in serum samples of healthy people was tested by the standard addition method under optimized conditions. As listed in Table 1, the results of spiking test were stable in the range of 98.27%–102.03%, indicating that the developed assay was viable to detect PLA_2 amount in actual samples, and showing potential in clinical test. To further evaluate the performance of the proposed LRET-based biosensor, after the conditions were optimized, then we used standard Lp-PLA_2 kit and our proposed biosensor to detect the amount of PLA_2 in the serums of healthy persons and different patients, respectively. As shown in Fig. 6C, the data show that the testing results of our proposed LRET-based biosensor are consistent with those of the standard Lp-PLA_2 kit. The PLA_2 content in normal human serum samples is lower than those in various patients, and the difference is approximately between 100–160 U/L. However, due to the small number of samples (n = 3), the results can't fully reflect the absolute law of data change, but it basically verifies that this analytical method can be initially applied to the detection of clinical samples.

4. Conclusions

In conclusion, a new LRET-based biosensor for detecting PLA_2 amount has been successfully developed. Therein, UCNPs act as prominent energy donor owing to their minimal autofluorescence and low background fluorescence, thus improving detection sensitivity. Furthermore, the fluorescence of SG can be enhanced upon its inserting to the small grooves of dsDNA, and the inserting leads to close proximity of energy donor and receptor. Through the LRET process from the UCNPs to the SG-dsDNA, the proposed assay has high sensitivity (LOD, 15 U/L) and wide linearity range (20–400 U/L) for the ratiometric fluorescence detection of PLA_2 amount. Therefore, this assay shows high specificity, and is successfully employed to

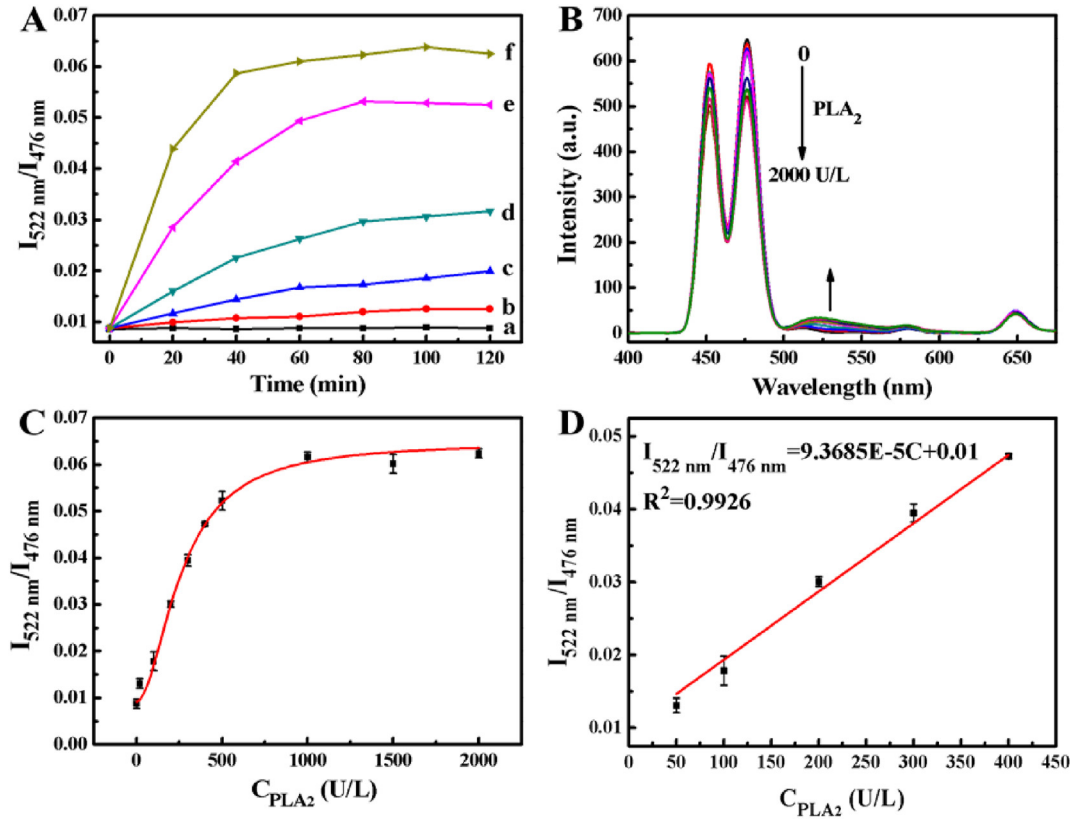

Fig. 5. (A) The $I_{522\ nm}/I_{476\ nm}$ ratio of UCNPs-SG nanoprobes after incubation with different concentrations of PLA_2 (a–f: 0, 20, 100, 200, 500, 1000 U/L) as a function of time. (B) UCL spectra of UCNPs-SG nanoprobes after incubation with different concentrations of PLA_2 (0, 20, 100, 200, 300, 400, 500, 1000, 1500, 2000 U/L). (C) The $I_{522\ nm}/I_{476\ nm}$ ratio as a function of PLA_2 amount. (D) Linear range of the plot of the $I_{522\ nm}/I_{476\ nm}$ ratio against PLA_2 amount (20–400 U/L). Error bars represent the standard deviations from three replicated experiments.

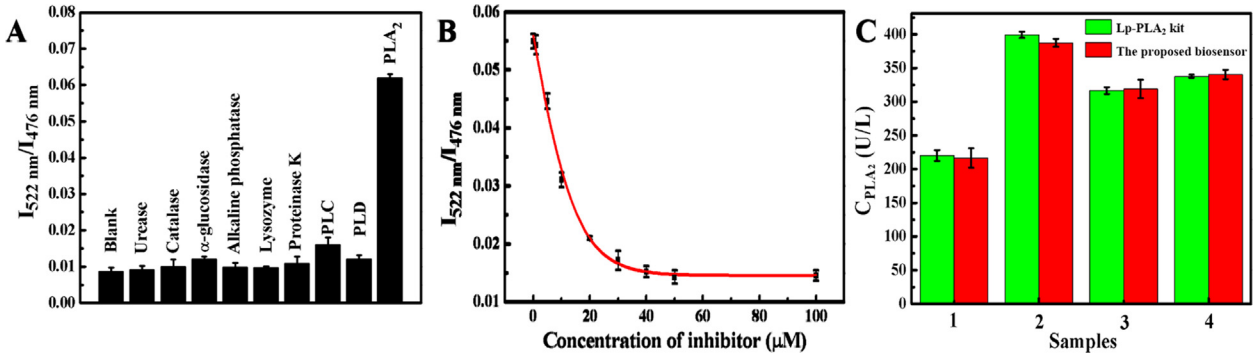

Fig. 6. (A) UCL responses of UCNPs-SG nanoprobes upon addition of other enzymes. The concentration of PLA_2 was 500 U/L, and the concentration of other enzymes was 1000 U/L. Error bars represent the standard deviations from three repeated experiments. (B) Dependence of the $I_{522\ nm}/I_{476\ nm}$ ratio on concentrations of inhibitor LY311727. Concentrations of inhibitor: 0, 1, 5, 10, 20, 30, 40, 50, 100 μM. The concentration of PLA_2 was 500 U/L. (C) The data of actual serum samples (1. healthy person, 2. pneumonia, 3. coronary heart disease, 4. cholelithiasis) tested by the Lp-PLA_2 kit (green) and the proposed LRET-based biosensor (red), respectively (n = 3). (For interpretation of the references to color in this figure legend, the reader is referred to the Web version of this article.)

Table 1
The spiking test of PLA_2 in human serum samples (n = 5).

Sample	Added (U/L)	Found (U/L)	Recovery (%)	RSD (%)
1	60	58.96	98.27%	1.28
2	150	153.04	102.03%	3.11
3	300	297.38	99.13%	2.34

detect the PLA_2 amount in actual samples. In addition, this research offers a great potential for enzyme inhibitor testing in clinical practice.

CRediT authorship contribution statement

Dengwang Luo: Conceptualization, Writing - original draft, Investigation. **Chaoyu Zhang:** Validation, Writing - original draft. **Yao Fang:** Data curation. **Yiping Shen:** Methodology. **Yuan Liang:** Methodology. **Yaokun Xia:** Methodology, Investigation. **Fang Wu:** Methodology, Data curation. **Xiaosong Chen:** Data curation. **Jingrong Liu:** Investigation, Methodology. **Jinghua Chen:** Funding acquisition, Writing - review & editing. **Chunyan Li:** Funding acquisition, Formal analysis, Writing - review & editing. **Jianming**

Lan: Conceptualization, Resources, Writing - review & editing, Funding acquisition, Supervision.

Declaration of competing interest

The authors declare that they have no known competing financial interests or personal relationships that could have appeared to influence the work reported in this paper.

Acknowledgments

This work was financially supported by the National Natural Science Foundation of China (21874019, 81971855), the Natural Science Foundation of Fujian Province (2019J01534, 2019J01680, 2019J01681, 2020J01628), the Provincial Joint Fund Project for Scientific and Technological Innovation-Grant (2017Y9101), and the Special Financial Funds of Fujian Province-Grant (2018B054).

Appendix A. Supplementary data

Supplementary data to this article can be found online at https://doi.org/10.1016/j.aca.2020.11.025.

References

[1] E.A. Dennis, J. Cao, Y.H. Hsu, V. Magrioti, G. Kokotos, Phospholipase A_2 enzymes: physical structure, biological function, disease implication, chemical inhibition, and therapeutic intervention, Chem. Rev. 111 (2011) 6130–6185.
[2] A.V. Lechuga-Vieco, H. Groult, J. Pellico, J. Mateo, J.A. Enriquez, J. Ruiz-Cabello, F. Herranz, Protein corona and phospholipase activity drive selective accumulation of nanomicelles in atherosclerotic plaques, Nanomed. Nanotechnol. Biol. Med. 14 (2018) 643–650.
[3] H.W.M. Niessen, P.A.J. Krijnen, C.A. Visser, C.J.L.M. Meijer, C.E. Hack, Type II secretory phospholipase A_2 in cardiovascular disease: a mediator in atherosclerosis and ischemic damage to cardiomyocytes? Cardiovasc. Res. 60 (2003) 68–77.
[4] N.J. Liu, R. Chapman, Y.Y. Lin, J. Mmesi, A. Bentham, M. Tyreman, S. Abraham, M.M. Stevens, Point of care testing of phospholipase A_2 group IIA for serological diagnosis of rheumatoid arthritis, Nanoscale 8 (2016) 4482–4485.
[5] A.J.J. Schrama, A.J. De Beaufort, B.J.H.M. Poorthuis, H.M. Berger, F.J. Walther, Secretory phospholipase A_2 in newborn infants with sepsis, J. Perinatol. 28 (2008) 291–296.
[6] M. Menschikowski, A. Hagelgans, S. Fuessel, O.A. Mareninova, V. Neumeister, M.P. Wirth, G. Siegert, Serum levels of secreted group IIA phospholipase A_2 in benign prostatic hyperplasia and prostate cancer: a biomarker for inflammation or neoplasia? Inflammation 35 (2012) 1113–1118.
[7] E. Kupert, M. Anderson, Y. Liu, P. Succop, L. Levin, J. Wang, K. Wikenheiserbrokamp, P.P. Chen, S.M. Pinney, T. Macdonald, Z.Y. Dong, T. Macdonald, Plasma secretory phospholipase A_2-IIa as a potential biomarker for lung cancer in patients with solitary pulmonary nodules, BMC Canc. 11 (2011) 513.
[8] D. Aili, M. Mager, D. Roche, M.M. Stevens, Hybrid nanoparticle-liposome detection of phospholipase activity, Nano Lett. 11 (2011) 1401–1405.
[9] R. Chapman, Y. Lin, M. Burnapp, A. Bentham, D. Hillier, A. Zabron, S. Khan, M. Tyreman, M.M. Stevens, Multivalent nanoparticle networks enable point-of-care detection of human phospholipase-A_2 in serum, ACS Nano 9 (2015) 2565–2573.
[10] Z. Cheng, A. Tsourkas, Monitoring phospholipase A_2 activity with Gd-encapsulated phospholipid liposomes, Sci. Rep. 4 (2014) 6958.
[11] C. Guo, Y. Zhang, Y. Li, S. Xu, L. Wang, ^{19}F-MRI nanoprobes for turn-on detection of phospholipase A_2 with low background, Anal. Chem. 91 (2019) 8147–8153.
[12] Y. Zhang, J. Ai, Y. Dong, S. Zhang, Q. Gao, H. Qi, C. Zhang, Z. Cheng, Combining 3D graphene-like screen-printed carbon electrode with methylene blue-loaded liposomal nanoprobes for phospholipase A_2 detection, Biosens. Bioelectron. 126 (2019) 255–260.
[13] F. Ghomashchi, B.Z. Yu, O. Berg, M.K. Jain, M.H. Gelb, Interfacial catalysis by phospholipase A_2: substrate specificity in vesicles, Biochemistry 30 (1991) 7318–7329.
[14] J. Aufenanger, W. Zimmer, M. Püttmann, R. Ensenauer, Determination of the catalytic activity of phospholipase A_2: E. coli-based assay compared to a photometric micelle assay, Eur. J. Clin. Chem. Clin. Biochem. 31 (1993) 777–785.
[15] C. Topbas, A. Swick, M. Razavi, N.L. Anderson, T.W. Pearson, C. Bystrom, Measurement of lipoprotein-associated phospholipase A_2 by use of 3 different methods: exploration of discordance between ELISA and activity assay, Clin. Chem. 64 (2018) 697–704.
[16] S.H. Chen, Y.P. Hsu, H.Y. Lu, J.A. Ho, Gold/phospholipid nanoconstructs as label-free optical probes for evaluating phospholipase A_2 activity, Biosens. Bioelectron. 52 (2014) 202–208.
[17] C. Zhang, Y. Yuan, S. Zhang, Y. Wang, Z. Liu, Biosensing platform based on fluorescence resonance energy transfer from upconverting nanocrystals to graphene oxide, Angew. Chem. Int. Ed. 50 (2011) 6851–6854.
[18] D.L. Scott, S.P. White, Z. Otwinowski, W. Yuan, M.H. Gelb, P.B. Sigler, Interfacial catalysis: the mechanism of phospholipase A_2, Science 250 (1990) 1541–1546.
[19] O. Wichmann, J. Wittbrodt, C. Schultz, A small-molecule FRET probe to monitor phospholipase A_2 activity in cells and organisms, Angew. Chem. Int. Ed. 45 (2006) 508–512.
[20] J. Li, Y. Zhang, J. Ai, Q. Gao, H. Qi, C. Zhang, Z. Cheng, Quantum dot cluster (QDC)-loaded phospholipid micelles as a FRET probe for phospholipase A_2 detection, RSC Adv. 6 (2016) 15895–15899.
[21] F. Zhou, B. Li, Exonuclease III-assisted target recycling amplification coupled with liposome-assisted amplification: one-step and dual-amplification strategy for highly sensitive fluorescence detection of DNA, Anal. Chem. 87 (2015) 7156–7162.
[22] B. Qu, L. Guo, X. Chu, D.H. Wu, G.L. Shen, R.Q. Yu, An electrochemical immunosensor based on enzyme-encapsulated liposomes and biocatalytic metal deposition, Anal. Chim. Acta 663 (2010) 147–152.
[23] J.A. Ho, W.L. Hsu, W.C. Liao, J.K. Chiu, M.L. Chen, H.C. Chang, C.C. Li, Ultrasensitive electrochemical detection of biotin using electrically addressable site-oriented antibody immobilization approach via aminophenyl boronic acid, Biosens. Bioelectron. 26 (2010) 1021–1027.
[24] A.I. Dragan, R. Pavlovic, J.B. McGivney, J.R. Casas-Finet, E.S. Bishop, R.J. Strouse, M.A. Schenerman, C.D. Geddes, SYBR Green I: fluorescence properties and interaction with DNA, J. Fluoresc. 22 (2012) 1189–1199.
[25] H. Zipper, H. Brunner, J. Bernhagen, F. Vitzthum, Investigations on DNA intercalation and surface binding by SYBR Green I, its structure determination and methodological implications, Nucleic Acids Res. 32 (2004) e103.
[26] S.C. Benson, R.A. Mathies, A.N. Glazer, Heterodimeric DNA-binding dyes designed for energy transfer: stability and applications of the DNA complexes, Nucleic Acids Res. 21 (1993) 5720–5726.
[27] C. Kanony, B. Åkerman, E. Tuite, Photobleaching of asymmetric cyanines used for fluorescence imaging of single DNA molecules, J. Am. Chem. Soc. 123 (2001) 7985–7995.
[28] X. Zhu, Q. Su, W. Feng, F. Li, Anti-Stokes shift luminescent materials for bioapplications, Chem. Soc. Rev. 46 (2017) 1025–1039.
[29] S. Wu, H.J. Butt, Near-infrared-sensitive materials based on upconverting nanoparticles, Adv. Mater. 28 (2016) 1208–1226.
[30] B. Zhou, B. Shi, D. Jin, X. Liu, Controlling upconversion nanocrystals for emerging applications, Nat. Nanotechnol. 10 (2015) 924–936.
[31] A.N. Vijayan, Z. Liu, H. Zhao, P. Zhang, Nicking enzyme-assisted signal-amplifiable Hg^{2+} detection using upconversion nanoparticles, Anal. Chim. Acta 1072 (2019) 75–80.
[32] H. Rabie, Y. Zhang, N. Pasquale, M.J. Lagos, P.E. Batson, K.B. Lee, NIR biosensing of neurotransmitters in stem cell-derived neural interface using advanced core-shell upconversion nanoparticles, Adv. Mater. 31 (2019) 1806991.
[33] K. Zhang, L. Yang, F. Lu, X. Wu, J.J. Zhu, A universal upconversion sensing platform for the sensitive detection of tumour-related ncRNA through an Exo III-assisted cycling amplification strategy, Small 14 (2018) 1703858.
[34] E.J. Jo, J.Y. Byun, H. Mun, D. Bang, J.H. Son, J.Y. Lee, L.P. Lee, M.G. Kim, Single-step LRET aptasensor for rapid mycotoxin detection, Anal. Chem. 90 (2018) 716–722.
[35] M. Wang, J.L. Liu, Y.X. Zhang, W. Hou, X.L. Wu, S.K. Xu, Two-phase solvothermal synthesis of rare-earth doped $NaYF_4$ upconversion fluorescent nanocrystals, Mater. Lett. 63 (2009) 325–327.
[36] A. Dong, X. Ye, J. Chen, Y. Kang, T. Gordon, J.M. Kikkawa, C.B. Murray, A generalized ligand-exchange strategy enabling sequential surface functionalization of colloidal nanocrystals, J. Am. Chem. Soc. 133 (2011) 998–1006.
[37] S.T. Proulx, P. Luciani, S. Derzsi, M. Rinderknecht, V. Mumprecht, J.C. Leroux, M. Detmar, Quantitative imaging of lymphatic function with liposomal indocyanine green, Canc. Res. 70 (2010) 7053–7062.
[38] L.L. Li, P. Wu, K. Hwang, Y. Lu, An exceptionally simple strategy for DNA-functionalized up-conversion nanoparticles as biocompatible agents for nanoassembly, DNA delivery, and imaging, J. Am. Chem. Soc. 135 (2013) 2411–2414.
[39] Y. Yang, K.M. Mayer, N.S. Wickremasinghe, J.H. Hafner, Probing the lipid membrane dipole potential by atomic force microscopy, Biophys. J. 95 (2008) 5193–5199.
[40] V. Muhr, C. Würth, M. Kraft, M. Buchner, A.J. Baeumner, U. Resch-Genger, T. Hirsch, Particle-size-dependent Förster resonance energy transfer from upconversion nanoparticles to organic dyes, Anal. Chem. 89 (2017) 4868–4874.